Journal of Solid State Chemistry 183 (2010) 2957–2962

Contents lists available at ScienceDirect

Journal of Solid State Chemistry

journal homepage: www.elsevier.com/locate/jssc

Two inorganic–organic hybrid materials based on polyoxometalate anions and methylene blue: Preparations, crystal structures and properties

Shanshan Nie [a], Yaobin Zhang [a], Bin Liu [a], Zuoxi Li [a], Huaiming Hu [a], Ganglin Xue [a,*], Feng Fu [b], Jiwu Wang [b]

[a] Key Laboratory of Synthetic and Natural Functional Molecule Chemistry (Ministry of Education), Shaanxi Key Laboratory of Physico-Inorganic Chemistry, Department of Chemistry, Northwest University, Xi'an 710069, China
[b] Department of Chemistry, Yanan University, Yan'an 716000, China

ARTICLE INFO

Article history:
Received 6 June 2010
Received in revised form
9 August 2010
Accepted 15 August 2010

Keywords:
Inorganic–organic hybrids
Polyoxometalates
Organic dye
Charge transfer

ABSTRACT

Two novel inorganic–organic hybrid materials based on an organic dye cation methylene blue (MB) and Lindqvist-type POM polyanions, $[C_{22}H_{18}N_3S]_2Mo_6O_{19}$ 2DMF **(1)** and $[C_{22}H_{18}N_3S]_2W_6O_{19}$ 2DMF **(2)** were synthesized under ambient conditions and characterized by CV, IR spectroscopy, solid diffuse reflectance spectrum, UV–vis spectra in DMF solution, luminescent spectrum and single crystal X-ray diffraction. Crystallographic data reveal that compounds **1** and **2** are isostructural and both crystallize in the triclinic space group $P\bar{1}$. Their crystal structures present that the layers of organic molecules and inorganic anions array alternatively, and there exist strong $\pi\cdots\pi$ stacking interactions between dimeric MB cations and near distance interactions among organic dye cations, Lindqvist-type POM polyanions and DMF molecules. The solid diffuse reflectance spectra and UV–vis spectra in DMF solution appear new absorption bands ascribed to the charge-transfer transition between the cationic MB donor and the POM acceptors. Studies of the photoluminescent properties show that the formation of **1** and **2** lead to the fluorescence quenching of starting materials.

1. Introduction

In recent years, investigation of inorganic–organic hybrid materials containing polyoxometalates (POMs) has attracted increasing attention because of the interesting synergistic effects among organic groups and POMs and application in medicine, non-linear optical materials and catalysis [1,2]. Polyoxometalates (POMs), as early transition-metal oxide clusters, have excited considerable interest in solid-state materials chemistry, because of their structural and compositional diversity, and great potential applications in catalysis, sorption, ion exchange, optical, electro and magnetic materials [1,3]. As electron-accepting moieties, POMs can combine with organic π-electron donors, such as planar tetrathiafulvalene (TTF) [3–6], planar arene donors (anthracenes and pyrenes) [7], ferrocenyl [8–12] and other rich electron organic molecules containing N, S, O atoms [13–16], most of these hybrids are stabilized by hydrogen bonding or Coulombic forces. The fabrication of hybrid, supramolecular systems based on the combination of organic dye cations and POM building blocks is also an expectant strategy to achieve the integration of functions. The organic dye cations have predominant UV–vis optical properties owing to large planar conjugated π systems, however, there were only a few reports on hybrid materials based on organic dyes and POMs, and the cocrystallization of the bulky spherical polyoxometalates with planar aromatic compounds represents an enormous experimental challenge owing to structural incompatibility of the two components [7,17]. The first hybrid containing triarylmethane dye, pararosaniline, $[(C_{19}H_{18}N_3)_2H][PMo_{12}O_{40}]$ was reported in 2002 [18]. Then $[C_{15}H_{17}N_4]_4[Mo_8O_{26}]$ based on neutral red was reported in 2005 [19]. Very recently, Xie [20,21] successfully synthesized $[C_{19}H_{18}N_3]_4[\alpha\text{-}S_2Mo_{18}O_{62}]$, $[C_{19}H_{18}N_3]_4[Mo_8O_{26}]$,8.5DMF, $[C_{19}H_{18}N_3]_6[MW_{12}O_{40}](M=Co, Zn, B)$ $[C_{22}H_{24}N_3]_4[SiW_{12}O_{40}]$. As part of our longstanding efforts in synthesizing inorganic–organic hybrid materials with potential synergistic properties, herein we report the synthesis, structure and properties of two new inorganic–organic hybrid materials based on Lindqvist-type anions and methylene blue, $[C_{22}H_{18}N_3S]_2Mo_6O_{19}\cdot 2DMF$ **(1)** and $[C_{22}H_{18}N_3S]_2W_6O_{19}\cdot 2DMF$ **(2)**. This is the first example of inorganic–organic hybrid material based on methylene blue and POMs. The planar methylene blue (MB) is expected some similarity with TTFs because it contains S atom in its planar framework and short $\pi\cdots\pi$ contacts which play an important role for the charge transfer transition [22].

2. Experimental

2.1. Materials and general methods

All materials were AR grade used as purchased. MB, acetonitrile and DMF were purchased from Tianjin Kermel Chemical

* Corresponding author. Fax: +86 029 88303798.
E-mail address: xglin707@163.com (G. Xue).

0022-4596/$ - see front matter © 2010 Elsevier Inc. All rights reserved.
doi:10.1016/j.jssc.2010.08.023

Reagents Co., Ltd., and $Na_2MO_4 \cdot 2H_2O$ (M=Mo, W) was obtained from Tianjin Basifu Chemical Reagents Co., Ltd. The $(NBu_4)_2[Mo_6O_{19}]$ and $(NBu_4)_2[W_6O_{19}]$ were prepared according to the literature procedures [23]. IR spectra were obtained on an EQUINOX55 IR spectrometer with KBr pellets. Solid state diffuse reflectance spectra between 200 and 850 nm were obtained for the dry pressed disk samples using a Shimazu UV-2550 spectrophotometer, equipped with an integrating sphere coated with polytetrafluoroethylene (PTFE). Absorption spectra were referenced to barium sulphate. Fluorescence spectra (FS) were measured at room temperature on a Hitachi F 4500 fluorescence spectrophotometer equipped with a 450 W xenon lamp as the excitation source. Cyclic voltammetry (CV) studies were carried out in DMF solution at ambient temperature under the protection of N_2 using an EG & G 273A apparatus. Calomel electrode was used as the reference electrode, and a platinum wire as the counter electrode. Potentials are quoted against a saturated calomel electrode (SCE). 0.1 M NBu_4Br as the supporting electrolyte, and the scan rate was 100 mV s^{-1}.

2.2. Synthesis

2.2.1. Synthesis of $[C_{22}H_{18}N_3S]_2Mo_6O_{19} \cdot 2DMF$ (**1**)

$(NBu_4)_2[Mo_6O_{19}]$ (0.14 g, 0.1 mmol) was dissolved in 15 mL of acetonitrile. To this solution methylene blue (0.075 g, 0.2 mmol) dissolved in 20 mL of distilled water was added with stirring. Then grey-purple precipitate appeared and filtered, the solid product was dissolved in 15 mL of DMF. After filtering, the dark-blue solution was allowed to stand in a closed container at r.t. Slow evaporation led to dark block crystals of **1**. Yield: 31% (based on Mo). Elemental analysis(%). Anal. calcd. for $C_{38}H_{50}N_8Mo_6O_{21}S_2$ (1594.62): C, 28.6; H, 3.2; N, 7.0; S, 4.0; Mo, 36.1%; Found: C, 29.1; H, 2.8; N, 6.4; S, 4.6; Mo, 35.5(%).

2.2.2. Synthesis of $[C_{22}H_{18}N_3S]_2W_6O_{19} \cdot 2DMF$ (**2**)

The procedure for **2** is similar to that of **1** except for using $(NBu_4)_2[W_6O_{19}]$ (0.19 g, 0.1 mmol) instead of $(NBu_4)_2[Mo_6O_{19}]$. Yield: 35% (based on W). Anal. calcd. for $C_{38}H_{50}N_8O_{21}S_2W_6$ (2122.01): C, 21.5; H, 2.4; N, 5.3; S, 3.0; W, 52.0%; Found: C, 21.0; H, 1.9; N, 4.6; S, 3.6; W, 52.8(%).

Table 1
Crystal data and refinement parameters for **1** and **2**.

Compound	**1**	**2**
Empirical formula	$C_{38}H_{50}N_8Mo_6O_{21}S_2$	$C_{38}H_{50}N_8O_{21}S_2W_6$
Formula weight	1594.62	2122.08
Temperature/K	296(2)	296(2)
Crystal system	triclinic	triclinic
Space group	$P\bar{1}$	$P\bar{1}$
a/Å	10.387(8)	10.368(18)
b/Å	11.682(9)	11.703(2)
c/Å	12.126(10)	12.164(2)
α/°	90.013(10)	89.777(2)
β/°	115.107(10)	65.197(2)
γ/°	100.474(10)	79.206(2)
V/Å^3	1305.17(18)	1311.4(4)
Z	1	1
μ/mm^{-1}	1.561	13.266
F(0 0 0)	786	978
Limiting indices	$-12 \le h \le 11$ $-11 \le k \le 13$ $-14 \le l \le 13$	$-9 \le h \le 12$ $-12 \le k \le 13$ $-14 \le l \le 14$
D_{calcl}/g cm^{-3}	2.029	2.687
GOF on F^2	1.047	0.988
$R1$, $wR2$ [$I > 2\sigma(I)$]	$R1$=0.0318, $wR2$=0.0829	$R1$=0.0499, $wR2$=0.1315
$R1$, $wR2$ (all data)	$R1$=0.0378, $wR2$=0.0897	$R1$=0.0616, $wR2$=0.1542

$R1 = [\Sigma|F_o| - |F_c|]/[\Sigma|F_c|]$. $wR2 = \{[\Sigma w(F_o^2 - F_c^2)^2]/[\Sigma w(F_o^2)^2]\}^{1/2}$.

2.3. Crystal structure determination

Crystal data and details of the data collection and refinement of compound **1** and **2** are summarized in Table 1. Data were collected on a BRUKER SMART APEX II CCD diffractometer with Mo$K\alpha$ monochromatic radiation (λ=0.71073 Å) at 296(2) K. The structure were solved by direct methods (SHELXTL-97) and refined by the full-matrix-block least-squares method on F^2. All non-hydrogen atoms were refined with anisotropic displacement parameters. Hydrogen atoms were included at calculated positions and refined with a riding model. Crystallographic data for the structures reported in this paper have been deposited in the Cambridge Crystallographic Data Center with CCDC reference numbers 778773 and 778772 for compounds **1** and **2**, respectively.

3. Results and discussion

3.1. Synthesis consideration

The crystalline $[C_{22}H_{18}N_3S]_2Mo_6O_{19} \cdot 2DMF$ **(1)** and $[C_{22}H_{18}N_3S]_2W_6O_{19} \cdot 2DMF$ **(2)** were obtained by recrystallizing the powdered precipitate, a product of reacting MB water solution with $(NBu_4)_2Mo_6O_{19}$ acetonitrile solution, in DMF solvent under the ambient conditions. In the process of synthesis, choosing a suitable solvent, especially for MB, is very important. We tried to dissolve the dye in ethanol or acetonitrile and react with MB aqueous or organic solution, no title compounds were isolated out, instead we got some POM crystals wrapped by dye.

3.2. Description of crystal structures

The crystal structure analysis reveals that **1** and **2** have the similar structure, and they all are crystallized in the triclinic space group$P\bar{1}$. So only the structure of compound **1** is discussed here. The asymmetric unit of **1** is composed of half of $Mo_6O_{19}^{2-}$, one MB cation and one DMF molecule and the ratio is 1:2:2 (Fig. 1). Each Lindqvist anion with the Mo–Oa, Mo–Ob and Mo–Oc average distances of 1.684, 1.910 and 2.230 Å, respectively, is surrounded by ten adjacent MB cations and four DMF molecules with the distances of C···O from 3.319 to 3.498 Å, which shows the

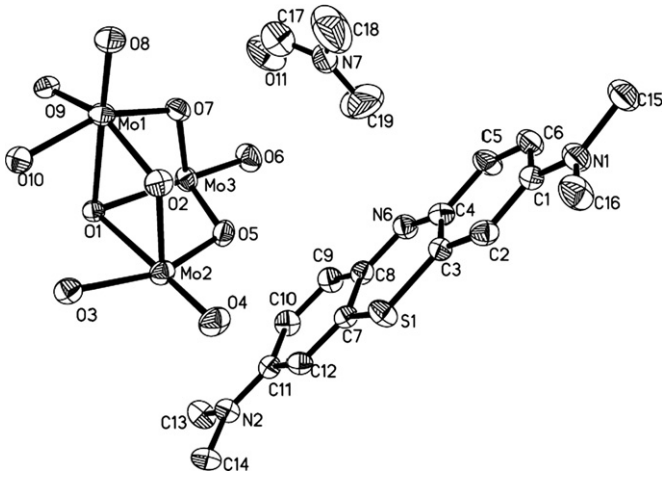

Fig. 1. ORTEP diagram of the asymmetric unit of **1** with the atomic numbering scheme and 30% thermal ellipsoids. H atoms are omitted for clarity.

presence of close interactions among the three components via Coulombic forces and C–H···O hydrogen bonds.

The crystal structure of $[C_{22}H_{18}N_3S]_2Mo_6O_{19}\cdot 2DMF$ **(1)** presents a 3D packing, the layers of the organic cations and inorganic anions are alternatively arranged in (0 0 1) planes (Fig. 2). There are two types of MB cations produced by symmetric operation, A and B, which are approximately parallel to each other with an angle of 1.51° and form a dimer with an interplanar distance ranging from 3.436 to 3.584 Å (mean 3.538 Å), and the nearest distance between the carbon atom of methyl of MB cation and the benzene ring of the next is 2.926 Å (Fig. 3), all of these demonstrated the presence of strong C–H···π interactions and face-to-face aromatic interactions in compound **1**. Furthermore the dimers self-assemble into the layers of the organic donor with DMF molecules by hydrogen bonding.

It is noticeable that the DMF molecules play an important role as nodes in constructing the supramolecular compound (Fig. 4). First, methyl of DMF molecule penetrate into the anion layers with the closest C···O distance of 3.333 Å and it bridges adjacent $Mo_6O_{19}^{2-}$ units via C–H···O hydrogen bonds into one-dimensional inorganic chains that run along *b*-axis. Second, DMF molecule also connects adjacent MB molecules via C–H···O hydrogen bonds. All of these led to the formation of hydrogen bonding cycles (Fig. 4) and construct a complex supramolecular network. The important role of DMF is in accord with the aforementioned synthesis, namely, they could be crystallized out in DMF solvent, rather than other organic solvents, such as ethanol or acetonitrile. Part hydrogen bond data in compound **1** are given in Table 2.

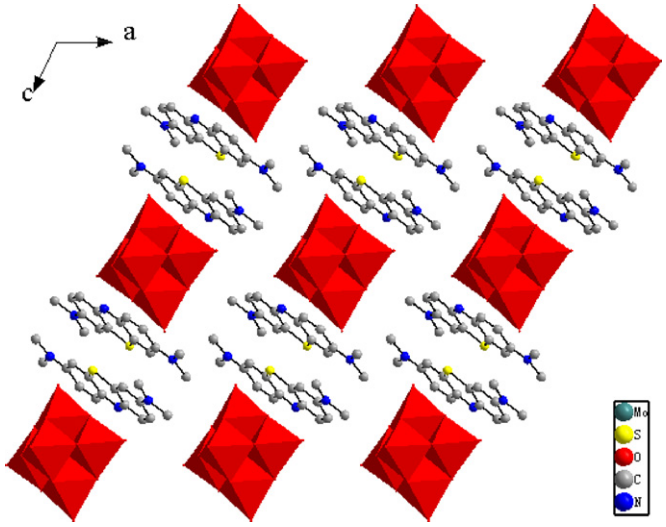

Fig. 2. The packing structure of compound **1**(H atoms and DMF molecules are omitted for clarity).

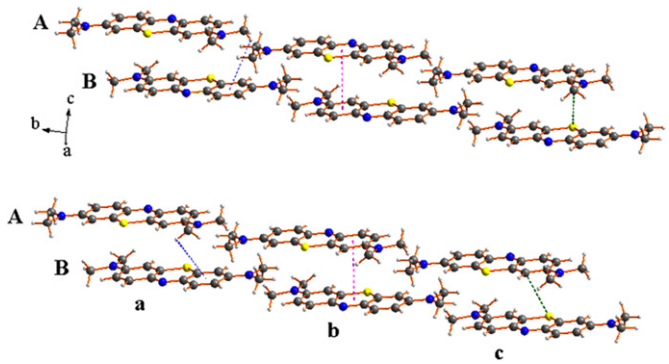

Fig. 3. A view of the parallel arrangement of A and B MB molecules in **1**. (a) C–H···π interactions. (b) face-to-face aromatic interactions. (c) short C–H…S contacts.

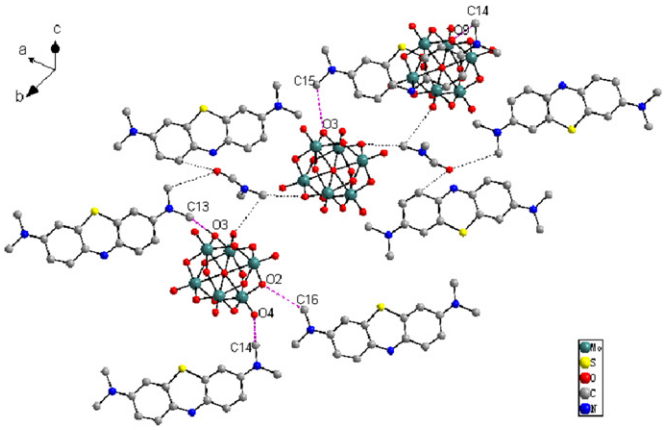

Fig. 4. A representation showing the hydrogen bonds among MB, DMF moleculars and $Mo_6O_{19}^{2-}$ in compound **1** (H atoms are omitted for clarity).

3.3. Characterization of compounds

3.3.1. IR spectra

The absorption peaks among $1000-3000\ cm^{-1}$ are mainly attributed to the characteristic peaks from methylene blue, and the peaks in the range 1000–600 cm^{-1} to those of the polyoxoanions. While the vibration frequencies of $\nu_{as}(M\text{–Oc})$ for **1** and **2** show slight changes, the $\nu_{as}(M\text{–Oa})$ and $\nu_{as}(M\text{–Ob})$ frequencies have a shift of 10–20 cm^{-1} compared with those of the starting materials due to the interaction among the organic dye cations and the framework oxygen atoms of polyoxometalates.

3.3.2. Solid diffuse reflectance spectra

The diffuse reflectance (UV–vis) spectra of hybrids **1** and **2** in comparison with the starting materials (MB, $[NBu_4]_2[M_6O_{19}]$ (M=Mo, W) are shown in Fig. 5. Compounds **1** and **2** (Fig. 5a and b, respectively) in the solid state exhibited a broad strong absorption band from 200 to 800 nm. Spectral (digital) subtraction of the component spectrum (i.e. of $[NBu_4]_2[Mo_6O_{19}]$ and MB, individually) of compound **1** in the solid state yielded the difference spectrum (Fig. 7a inset) consisting of a very climbing band from 500 nm and down trended at 750 nm. The diffuse reflectance spectrum of the salt **2** in the solid state (Fig. 7b) was similar to compound **1**, except the climbing band started from 450 nm. The observation is similar to those of the reported related charge-transfer salts [11,24], and the new (visible) absorption bands, according to Mulliken theory [25,26], could be ascribed to charge-transfer transitions between the cationic MB donor and the POM acceptor.

3.3.3. UV–vis spectra in DMF solution

UV–vis spectra of **1**, **2** and starting materials in DMF solution are shown in Fig. 6. Methylene blue possessed a significant absorption band at 665 nm and a less strong band at 294 nm. $[NBu_4]_2[Mo_6O_{19}]$ and $[NBu_4]_2[W_6O_{19}]$ had a weak absorption peak at 264 and 276 nm, respectively, and had no visible absorbance. The UV–vis spectrum of **1** shown in Fig. 6a represented four peaks, the bands within the UV range at 250 and 294 nm should be ascribed to organic dye or $[Mo_6O_{19}]^{2-}$ absorptions, the sharpest one in 665 nm in visible range was undoubtedly ascribed to methylene blue, and the most interesting

Table 2
Hydrogen bonds parameters in compound **1.**

D–H…A	d(D–H)/Å	d(H…A)/Å	d(D…A)/Å	∠DHA	A
C14–H14…O9	0.960	2.481	3.319	145.76	O9[x, $-1+y$, z]
C13–H13…O3	0.959	2.505	3.364	148.99	O3[$-x+1$, $-y+2$, $-z+1$]
C14–H14…O4	0.960	2.565	3.416	147.77	O4[x, $y+1$, z]
C15–H15…O3	0.960	2.575	3.435	149.11	O3[$-x+1$, $-y+1$, $-z+1$]
C16–H16…O2	0.960	2.609	3.498	154.22	O2[x, $y+1$, z]

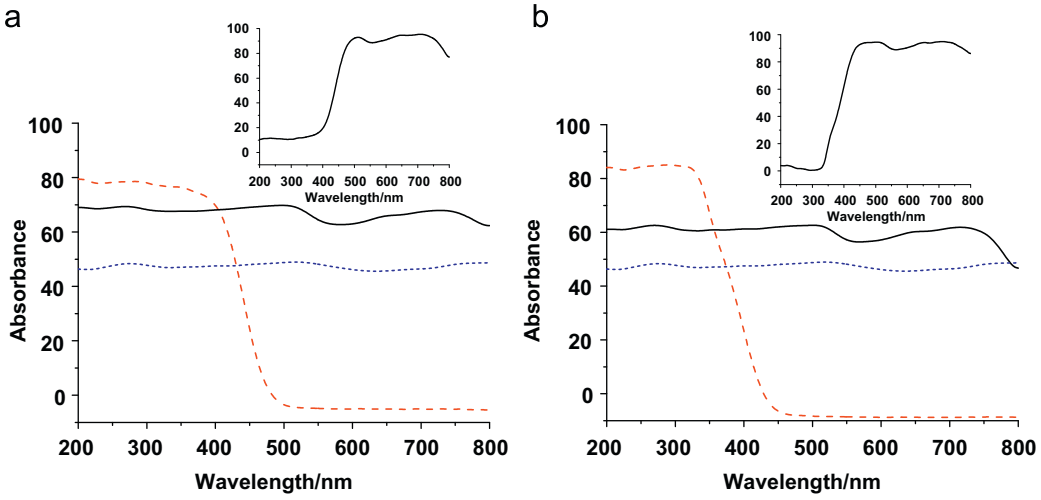

Fig. 5. Diffuse reflectance spectra of compound 1 (a) and 2 (b) (——) dispersed in barium sulfate in comparison with the absorption spectra of $[NBu_4]_2[M_6O_{19}]$ (M=Mo, W) (———), respectively, and MB(……). The inset elicits the charge-transfer band by the spectral (digital) subtraction of $[NBu_4]_2[M_6O_{19}]$ and MB individually from 1 or 2, respectively.

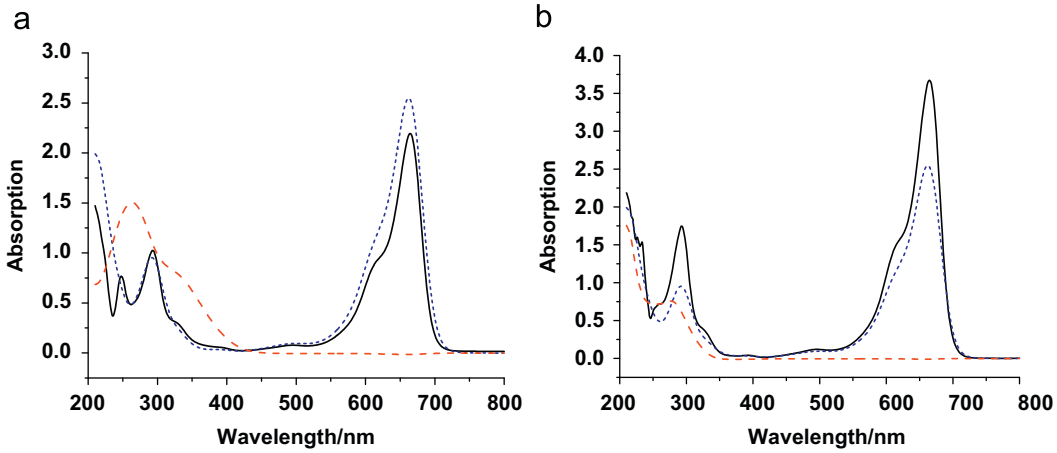

Fig. 6. UV–vis spectrum of **1**(a) and **2**(b)(——) dissolved in DMF(1.0×10^{-5} M) in comparison with the absorption spectra of $[NBu_4]_2[M_6O_{19}]$ (M=Mo, W) (———), respectively, and MB (……).

one is the fourth, which is a new shoulder peak located at about 615 nm and could be ascribed to the formation of ion pairs of $Mo_6O_{19}^{2-}$ anion and MB cation or charge-transfer transitions between the cationic MB donor and the POM acceptor in DMF solution. For compound **2**, the attention is focused on the new absorption band in visible range, similarly, a shoulder peak appeared at about 612 nm (Fig. 6b).

3.3.4. *Cyclic voltammetry*

The voltammetry curves (as shown in Fig. 7) of compounds **1** and **2** were measured in 1×10^{-4} mol/L DMF solution (0.1 M NBu_4Br as the supporting electrolyte). Compound **1** showed two pairs of redox waves, one at $E_{1/2}=-0.154$ V was attributed to methylene blue compared with that of free MB at -0.208 V, the other one in $E_{1/2}=-0.440$ V could be assigned to $[Mo_6O_{19}]^{2-}$ compared with that of $[NBu_4]_2[Mo_6O_{19}]$ at -0.452 V. For compound **2**, the redox wave of organic moiety appears in $E_{1/2}=-0.198$ V and that of $[W_6O_{19}]^{2-}$ at $E_{1/2}=-0.836$ V. The order of the reduction potentials with $E_{1/2}(Mo_6O_{19}^{2-})>E_{1/2}(W_6O_{19}^{2-})$ was consistent with the spectral extension of the hexamolybdate compound **1** from 500 nm compared with the hexatungstate compound **2** from 450 nm in the solid diffuse reflectance spectra [27]. The potential of organic donor in compounds **1** and **2** became more positive, which is similar to that of the charge-transfer salts [24] and suggest the formation of ion pairs of $Mo_6O_{19}^{2-}$ anion and

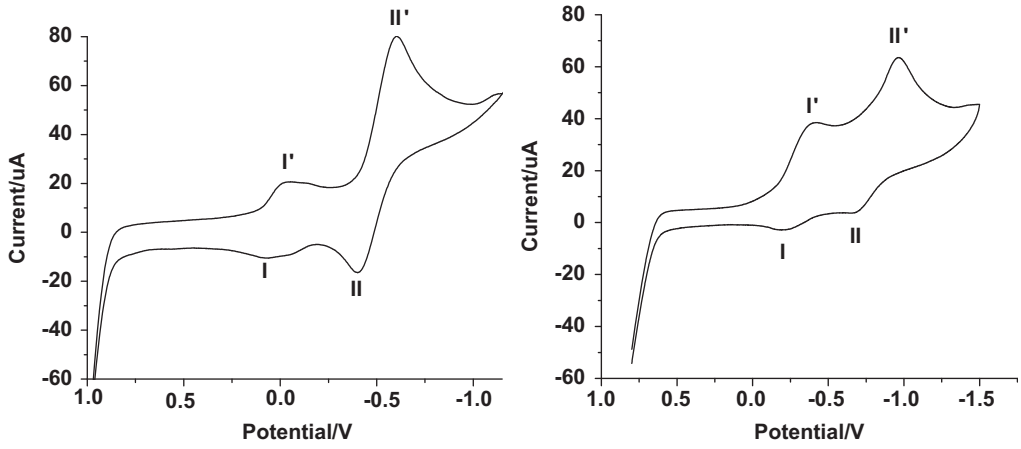

Fig. 7. Cyclic voltammetry of compound **1**(left) and **2**(right).

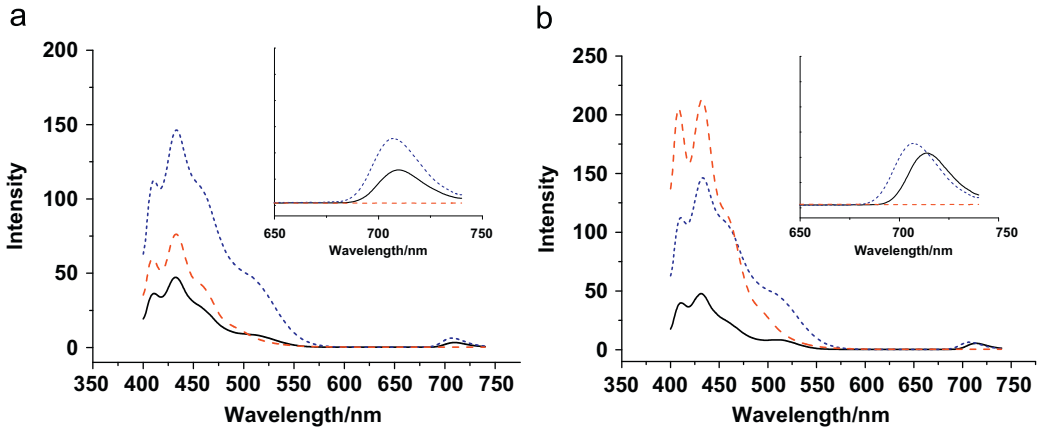

Fig. 8. Fluorescence emission spectra of **1**(a) and **2**(b)(——) dissolved in DMF (3.0×10^{-5} M) in comparison with the absorption spectra of $[NBu_4]_2[M_6O_{19}]$ (M=Mo, W) (———), respectively, and MB (……)(excitation wavelength 380 nm).

MB cation or charge-transfer transitions between the cationic MB donor and the POM acceptor in DMF solution.

3.3.5. *Fluorescence properties*

The fluorescence spectra of **1**, **2** and corresponding starting materials are recorded in 3.0×10^{-5} M DMF solution at room temperature (Fig. 8a and b). With excitation at 380 nm, all the emission peaks of compounds **1** or **2** between 400 and 550 nm distinctly decreased compared with those of the starting materials. Fig. 8a inset showed that compound **1** has a luminescent peak with a maximum at 709 nm assigned to that of methylene blue, which was also reduced and the wavelength redshifted 3 nm. Similar to **1**, compound **2** (Fig. 8b inset) showed an emission peak at 714 nm, the intensity reduced a little and the wavelength redshifted 8 nm. Obviously, all of these changes are owing to the interaction between MB and the polyanions in DMF solution and may suggest the occurrence of the charge transfer process between the MB donor and Lindqvist acceptors [28–30].

4. Conclusion

In summary, two novel inorganic–organic hybrid materials containing organic dye and POMs were prepared. Their crystal structures present the alternative arrangements of organic layers which are composed of MB dimers and DMF molecules and inorganic layers. The diffuse reflectance spectra of **1** and **2** show the charge-transfer absorption band between the cationic MB donor and the POM acceptor. UV–vis spectra in DMF solution also appear charge-transfer absorption band between the cationic MB donor and the POM acceptor. Studies of the photoluminescent properties show the formation of **1** and **2** lead to the fluorescence quenching of starting materials. This paper verifies that the conjugated MB dye molecules can be used as organic cations to synthesis inorganic–organic hybrid materials. Further study is underway to get more related compounds with organic dyes and the valuable properties of these compounds are being pursued.

Acknowledgments

This work was supported by the National Natural Science Foundation of China (20973133), the Education Commission of Shaanxi Province (09JK783) and the National Training Fund for the basic sciences (J083417/J0104).

Appendix A. Supporting information

Supplementary data associated with this article can be found in the online version at doi:10.1016/j.jssc.2010.08.023.

References

[1] C.L. Hill, Chem. Rev. 98 (1998) 1–2 Ed..
[2] M. Clemente-León, E. Coronado, C.J. Gómez-García, E. Martinez-Ferrero, J. Clust. Sci. 13 (2002) 381–407.

[3] E. Coronado, J. Gómez-García, Chem. Rev. 98 (1998) 273–296.
[4] E. Coronado, C. Giménez-Saiz, C.J. Gómez-García, J. Coord. Chem. Rev. 249 (2005) 1776–1796.
[5] E. Coronado, C. Giménez-Saiz, C.J. Gómez-García, S.C. Capelli, Angew. Chem. Int. Ed. 43 (2004) 3022–3025.
[6] J. Peng, E.B. Wang, Y.S. Zhou, Y. Xing, H.Q. Jia, Y.H. Lin, Y.G. Shen, J. Chem. Soc., Dalton Trans. (1998) 3865–3870.
[7] P. Le Maguerès, S.M. Hubig, S.V. Lindeman, P. Veya, J.K. Kochi, J. Am. Chem. Soc. 122 (2000) 10073–10082.
[8] J.S. Miller, A.J. Epstein, W.M. Reiff, Chem. Rev. 88 (1988) 201–220.
[9] P.L. Maguerès, L. Ouahab, S. Golhen, D. Grandjean, O. Peña, J.C. Jegaden, C.J. ómez-García, P. Delhaès, Inorg. Chem. 33 (1994) 5180–5187.
[10] Z.F. Li, R.R. Cui, B. Liu, G.L. Xue, H.M. Hu, F. Fu, J.W. Wang, J. Mol. Struct. 920 (2009) 436–440.
[11] Z.F. Li, B. Liu, H.S. Xu, G.L. Xue, H.M. Hu, F. Fu, J.W. Wang, J. Organomet. Chem. 694 (2009) 2210–2216.
[12] Z.F. Li, R.R. Cui, G.L. Xue, H.M. Hu, F. Fu, J.W. Wang, J. Coord. Chem. 62 (2009) 1951–1958.
[13] L.J. Zhang, Y.S. Zhou, Z. Yu, G.S. Fang, X.Z..You, 570 (2001) 83–90.
[14] J.H. Liu, J. Peng, E.B. Wang, L.H. Bi, S.R. Guo, J. Mol. Struct. 525 (2000) 71–77.
[15] D.C. Crans, M. Mahroof-Tahir, O.P. Aderson, M.M. Miller, Inorg. Chem. 33 (1994) 5586–5590.
[16] Z.G. Han, Y.L. Zhao, J. Peng, A.X. Tian, Y.H. Feng, Q. Liu, J. Solid State Chem. 178 (2005) 1386–1394.
[17] M.M. Olmstead, D.A. Costa, K. Maitra, B.C. Noll, S.L. Phillips, P.M. Van Calcar, A.L. Balch, J. Am. Chem. Soc. 121 (1999) 7090–7097.
[18] G. Liu, Q. Li, S.W. Zhang, Z. Anorg. Allg. Chem. 628 (2002) 1895–1898.
[19] Q. Li, S.W. Zhang, Z. Anorg. Allg. Chem. 631 (2005) 645–648.
[20] J.L. Xie, B.F. Abrahams, A.G. Wedd, Chem. Commun. (2008) 576–578.
[21] J.L. Xie, J. Coord. Chem. 61 (2008) 3993–4003.
[22] C. Rovira, Chem. Rev. 104 (2004) 5289–5317.
[23] W.G. Klemperer in: A.P. Ginsberg (ed.), Wiley, New York, 27 (1990) 77, 80.
[24] P.L. Veya, J.K. Kochi, J. Organomet. Chem. 488 (1995) C4–C8.
[25] R. Foster, in: Organic Charge-Transfer Complexes, Academic, New York, 1969.
[26] R.S. Mulliken, W.B. Person, in: Molecular Complexes. A Lecture and Reprint Volume, Wiley, New York, 1969.
[27] P.L. Maguerès, S.M. Hubig, S.V. Lindeman, P. Veya, J.K. Kochi, J. Am. Chem. Soc. 122 (2000) 10073–10082.
[28] M.K. Seery, L. Guerin, R.J. Forster, E. Gicquel, V. Hultgren, A.M. Bond, A.G. Wedd, T.E. Keyes, J. Phys. Chem. A. 108 (2004) 7399–7405.
[29] Y.W. Lu, B. Keita, L. Nadjo, G. Lagarde, E. Simoni, G.J. Zhang, G.A. Tsirlina, J. Phys. Chem. B. 110 (2006) 15633–15639.
[30] T.E. Keyes, E. Gicquel, L. Guerin, R.J. Forster, V. Hultgren, A.M. Bond, A.G. Wedd, Inorg. Chem. 42 (2003) 7897–7905.